

# Experimental characterization of a solar dryer and modelling of the drying kinetics of millet pellets

Soumaïla TIGAMPO, El Hadji I CISSE, Ababacar THIAM, Panel Thierry BASSENE, Vincent SAMBOU

**Abstract** - This paper an experimental evaluation of the performance of a mixed forced convection solar dryer and a modelling of the drying kinetics of millet pellets. The solar dryer has been characterized under no load and load conditions with millet pellets (*Pennisetum Glaucum*). Air temperature values of up to 48.8 °C have been obtained in the solar no load, a difference of 21.5 °C with the outside air temperature. A stratification of the air temperature has been observed in the drying chamber, reaching a maximum value of 6.9 °C. When drying millet pellets, the air temperature in the drying chamber has a maximum value of 34.4 °C, a difference of 13.4 °C with the outside air temperature. There is a reversal of air temperature and product drying rate between the trays in the mixed solar dryer with load. The characterization of solar dryer with loaded product consists of testing the dryer with 7 kg of millet pellets mass. The product has been dried for 5 hours, passing from an initial water content of 70% to a final water content of 5.2% (g of water/g of dry matter). Thin-layer mathematical models have been compared to observations of drying of millet pellets. The Page model found to be the best for millet drying pellets for samples from trays 1, 7 and 14 with correlation coefficients of  $R^2 = 0.9895$ ,  $R^2 = 0.9908$  and  $R^2 = 0.9825$ , respectively.

**Keywords:** solar dryer, characterization, millet pellets, modelling.

## Nomenclature

a, b, c, g, h, n	Empirical constants in drying models
k, k <sub>0</sub> , k <sub>1</sub>	Empirical coefficients in drying (s <sup>-1</sup> )
n	Number constant
N	Number of observation
m	Mass of the product (kg)
m <sub>d</sub>	Dry matter of the product (kg)
m <sub>t</sub>	Mass at the time t
R <sup>2</sup>	Coefficient of determination
RMSE	Root mean square error
T	Temperature (°C)
t	Time (hour)
M <sub>eq</sub>	Moisture content is an equilibrium state (dry basis)
M <sub>0</sub>	Moisture content at (t = 0)
M <sub>t</sub>	Moisture content at t (dry basis)
MR	Moisture ratio
DR	Drying rate, (kg/kg h <sup>-1</sup> )
MR <sub>exp</sub>	Experimental moisture ratio
MR <sub>pre</sub>	Predicted moisture ratio
σ <sup>2</sup>	Mean of the sum of the squared errors

## I. Introduction

Food self-sufficiency is one of the main challenges for emerging countries. Thus, the public authorities are strongly encouraging local cereal crops. This is the case of pearl millet (*Pennisetum Glaucum*), which the production is rising up. Millet is the staple food of

populations south of the Sahara. It is consumed in the form of couscous, porridge, semolina, and flour pellets in Africa. During the last two decades, the consumption of millet-based foods has increased sharply in Africa; and processing is an important element in the millet value chains. Thus, there are several SMEs (small and medium-sized enterprises) involved in the processing and marketing of millet-based products. Drying is an essential link in the processing of millet.

In recent years, a number of mechanical dryers have been developed that operate on various energy sources (electricity, gas, etc.). These types of dryers consume a significant amount of energy, which is becoming increasingly problematic with the soaring oil prices on the one hand and the environmental problems caused by the use of fossil resources on the other. The electrically heated system had a minimum energy consumption of 3.83 kW.h, while the convection gas dryer had a minimum energy consumption of 0.82 kW.h at 60 °C and 1.0 m/s [1]. As a result, the cost of drying will be relatively high due to rising fuel prices. Solar dryers are technologies that can convert the electromagnetic radiation emitted by the sun into heat. This heat is then transmitted to the food to extract the humidity. Introducing solar dryers in these SMEs makes it possible to have quality products with lower energy expenses. Solar dryers are proving to be a particularly interesting solution in our tropical countries. In many of our developing countries, the sun is an abundant, renewable, free and inexhaustible or power source. In addition, solar energy is one of the renewable energy sources with a low environmental impact [2]. In Senegal, particularly in Dakar, the solar potential is very high, about 5.8 kWh/m<sup>2</sup>/day for an average sunshine duration of 3,000 hours per year [3].

According to the mode of use of solar energy, solar dryers are generally classified into three categories: direct, indirect, and mixed. The direct solar dryer is a device in which the product is exposed directly to solar radiation. On the other hand, the product is dried by air previously heated in a solar collector in the indirect solar dryer. It protects the products to be dried from direct sunlight. Indirect drying can better preserve the product's color, nutritional quality, and physical appearance of the product. Thus, to increase the drying performance of agricultural products, the combination of the direct solar dryer and the indirect solar dryer gives the mixed solar dryer. It is more suitable for drying millet-based products which do not need to be protected from direct sunlight. Air circulation through the dryers is ensured by natural convection (passive mode) or forced convection (active mode).

In this work, it is a question of making an experimental characterization of the mixed dryer and studying the kinetics of drying the millet pellets. Several studies have focused on the airflow in dryers, which is the major factor affecting the overall efficiency of these devices. Afriye *et al.* [4] believe that natural

convection in dryers leads to poor ventilation with often excessive temperatures in the drying chamber, leading to biological, chemical, and mechanical alterations of the product to be dried. To improve natural convection, chimneys were introduced in passive solar dryers. Ekechukwu *et al.* [5] evaluated the natural air circulation induced by a 5.3 m high solar chimney. The results showed that a well-designed solar chimney could improve buoyancy-induced airflow. Better performance was obtained with a chimney with solar radiation absorbing surface. H. Krabch *et al.* [6] compared the thermal performance of three passive indirect solar dryers. The first solar dryer Dry1, has two components: a solar collector and a drying chamber. The second Dry2, has two compartments. The lower part is double-glazed, on which the drying chamber is placed. The third solar dryer, called Dry3, has only one compartment with absorbent materials on the sides. The experimental results showed high internal temperatures in Dry3 of the order of 40 °C compared to the other two dryers with a chimney. The average internal temperature in Dry1 is 34 °C and in Dry2 is 28 °C. Kumar *et al.* [7] studied a solar dryer with a vertical chimney collector for drying paddy rice. The experiments showed an increase in average air temperature from 21.8 °C to 27.1 °C, respectively, for the inclined collector and the vertical collector, with an average airflow of 0.22 m/s through the fireplace. A 33% reduction in airflow was observed in the dryer when the average air temperature in the tilted collector reached 68.5 °C. The 20 kg of paddy rice were dried for a period of 9 hours, going from an initial water content of 31% to 13% (dry basis), a saving of 7 hours over in the open air drying. They claim that the system can generate enough warm airflow to improve the drying rate with a vertical chimney collector. Ferreira *et al.* [8] showed the technical feasibility of a solar chimney for drying products. To evaluate this drying device, parameters such as air velocity, temperature and humidity were monitored as a function of sunlight. The results showed an increase in the air stream's temperature generated by the stack of  $13 \pm 1$  °C on average per year compared to the ambient air. To dry a capacity of approximately 440 kg of product, an average annual mass flow of  $1.40 \pm 0.08$  kg/s was observed. A. Fudholi *et al.* [9] conducted itemized review of the types of dryers for various agricultural and fishery products. They studied different solar dryers, considering the nature of the product to be dried, the technical aspects, and the economic costs. They showed that solar dryers have higher efficiency with the integration of solar collectors. Pruegam *et al.* [10] proposed a double-sided solar collector dryer for banana drying. They incorporated a 2 m high chimney at the end of the drying chamber to improve natural convection flow. This dryer reduces the drying time of the banana by a factor varying from 1.3 to 1.5 compared to drying in the open air. They pointed out that this solar dryer can produce more hot air with a very low relative humidity than air drying. On the other hand, the drying is carried out in active mode thanks to the fans powered by photovoltaic modules. A. Elkhadroui *et al.* [11] proposed a novel mixed-mode solar dryer with forced convection for drying red pepper slices. This drying system shortens the drying time by 7 hours compared to air drying. The average efficiency of the solar collector was found to be 57%, with a mass airflow of 0.047 kg/s. Al-Juamily *et al.*

[12] tested a fan-forced convection solar dryer for drying fruits and vegetables in Iraq. It involved the drying of grapes, apricots and beans. The grapes were dried for 85 hours, from an initial water content of 80% to a final water content of 18%, while the apricots were reduced to a final water content of 13% from their initial water content of 80% in 40 hours. The beans were dried for 20 hours, going from an initial content of 65% to a final content of 18%. These results were obtained with a constant airspeed of 0.4 m/s in the solar dryer.

M.S. K Asnaz *et al.* [13] evaluated the performance of different types of dryers. They designed a solar dryer that can be converted into three other dryer systems when needed. First, a natural convection dryer (CND) consisting of a solar collector, a drying chamber and a chimney was designed. Then two fans have been added to this design to have a forced convection dryer (FCD). These fans are powered by photovoltaic solar energy. The third option was to use a heat pump (HPD) that supplies hot, dry air to the collector and the drying chamber. The results showed that the temperature range inside the HPD chamber is higher than that of other FCD, and CND dryers, with respective temperatures of 45.7 °C, 43.8 °C and 42.8 °C. The highest efficiency is that of HPD, equal to 85.99% at 12:00 p.m., then that of FCD, equal to 78.36% at 2:00 p.m. and finally CND, equal to 68.97% at 12:00 p.m.

V. Subbian *et al.* [14] experimentally analyzed forced air circulation in a mixed solar dryer. The results showed that for a mass flow of 0.009 kg/s, the average drying air temperature was 44 °C. A maximum drying air temperature of 71 °C was recorded during peak sunlight hours.

H. S. El Mesery *et al.* [15] have analyzed the performance of three flow distribution systems for hot air in dryers. The first system is vertical (VS), in which the hot air passes vertically through the sample tray. The other two systems are horizontal, one with a single HS air inlet (I) and the other with three inlets (HS II). The air was distributed parallel to the sample tray. The results show that the drying time in HS (II) was significantly lower than in HS (I) and VS. This is because air flowing horizontally over the sample surface has a longer time than air flowing vertically through a thin layer.

V. Reddy Mugi *et al.* [16] compared the effect of forced convection and natural convection in a solar dryer. The results showed that the average temperature inside the drying chamber varied from 50.9 °C to 56.1 °C in natural convection, while in forced convection, it varied from 46.2 °C to 50.55 °C. Air temperature stratification in the dryer showed that the air temperature decreased from the lower to the upper position of the trays as the hot air exchanged its heat with the products while flowing to the other trays. The average efficiency in forced convection was 63.3%, while it was 53.84% in natural convection, a decrease of 17.53%.

Several experimental researches and mathematical modelling have been carried out on different products' thin-film solar drying process. M. Rezaei *et al.* [17] studied thin-layer drying of parsley in a forced convection solar dryer in the open air. The results showed that in 4.5 hours, the water content of parsley was reduced in the dryer, while it took about 3 days to reach the same water content when the parsley was shade dried in the open air. The experimental data were fitted with nine models of

drying kinetics by determining the RMSE and the  $R^2$ . The Midilli model has been found to provide accurate estimates for parsley drying in a solar dryer.

Several tests were carried out on dryers with different products to study the kinetics of thin layer solar drying. Several semi-empirical models have been proposed, and each mathematical model can describe a product's thin layer drying kinetics. N.F. Beye *et al.* [18] performed mathematical modelling of the kinetics of four varieties of Senegalese onions in an oven in the temperature range of 50 °C to 70 °C and in a greenhouse dryer. The results showed that the characteristic drying curves are identical for the four onion varieties and are described with third-order polynomials in the range of reduced water content from 0.1 to 0.7%. Nine empirical mathematical models were tested to model the drying kinetics in thin layers of the four onion varieties. The model parameters are estimated by non-linear regression. The two best models describing the drying kinetics of four onion varieties are the Page models and the Verma *et al.*

P.T. Bassene *et al.* [19] studied the modelling of the kinetics of drying in thin layers of millet pellets. This thin layer drying kinetics was studied in a controlled environment with an experimental device called a drying chamber using an air blower. Millet pellets were dried with different temperatures (40, 50 and 60 °C) and at a constant speed of 1.0 m/s. Ten mathematical models were tested to model millet pellets thin layer drying kinetics. Of these models, the modified model of Henderson and Pabis was the best for describing the thin layer drying kinetics of millet pellets in a drying vein. Other products have been investigated. K. Mugodo *et al.* [20] studied the kinetics of thin-layer drying of mango slices in a convective oven (OVD), in the open air (UAD) and in a greenhouse (MVD). The experiments were conducted on mango slices with thicknesses of 3 mm, 6 mm and 9 mm. The drying time decreased significantly for the thickness of 3 mm. Midilli *et al.* provided the most accurate model for describing the drying kinetics of mango slices. Turban [21] compared the kinetics of pepper drying in the open air and greenhouse-type solar dryers. P. Nimnuan and S. Nabnean [22] conducted an experimental and theoretical study of the performance of a solar dryer for ginger drying. S. Gasa *et al.* [23] modelled the thin layer drying of sweet potato slices in a hot air oven and a solar venturi dryer using several models.

There has never been researching to our knowledge done on millet pellets drying in a thin layer using a combination of solar energy and forced convection. In addition, there is no reported study on the phenomenon of reversal of air temperature and product drying rate between trays inside a mixed solar dryer with load. Thus, in this paper, we shall first provide the experimental characterization results of a solar dryer without product (without load). Next, we will present the results of the characterization of the solar dryer with load of millet pellets to determine the drying kinetics of these millet pellets. Finally, we will test mathematical models by a non-linear regression analysis describing the kinetics of drying in thin layers. For that, we will load all trays and test for three samples trays in different positions of the solar dryer, which are: the sample from tray 1, which is at the blowing door of the solar collector, the sample from tray 7, which is in the middle and the sample of tray 14 positioned on top.

## II. Materials and methods

### II.1. Description of the experimental device

The experimental study was carried out on a mixed forced convection solar dryer installed in Dakar, Senegal, at latitude 14° 41'37 N and longitude -17°26'38 W.

The solar dryer is divided into two zones: the solar heating zone (solar collector) which is composed of the absorber, the glass, the ventilator and the insulation for the back glass losses and the drying zone, where the product (millet) is exposed. This last zone comprises the drying trays, the glass, the chimney, and the door for filling the products. A photograph of the mixed solar dryer is presented in figure 1. This drying system has a total drying surface of 7.84 m<sup>2</sup>.



Figure 1: Photograph of the solar dryer

#### II.1.1. The solar collector

The solar collector is the air heating zone. It consists of an absorber of dimensions (length 1.7 m, width 0.8 m, thickness 0.105 m), a transparent glass cover of 6 mm thickness and the same dimension as the absorber. The absorber is made of steel sheet painted in matt black with an emissivity of 0.95 and an absorption coefficient of 0.8. Polyurethane is used to insulate the collector's sides and rear. An air gap value between the glass cover and the absorber is 0.0035mm, between which the drying air is blown by two fans powered by a photovoltaic module. The solar collector is south-facing with an inclination of 15° to the horizontal plane

#### II.1.2. Drying chamber

The Drying chamber is parallelepipedic with the following dimensions length 0.98 m, width 0.78 m and height 2.3 m. It is surmounted by a chimney to improve the evacuation of the humid air. The different components are shown in Figure 2. The vertical walls and the roof of the drying chamber are made of 6 mm thick transparent glass. The dryer can contain 14 trays on which the products to be dried are spread out. The trays' dimensions are 0.80 m x 0.70 m; The trays are 11 cm apart to facilitate airflow. The drying chamber is placed on a concrete support length of 0.96 m, a width of 0.75 m and a height of 0.26 m.

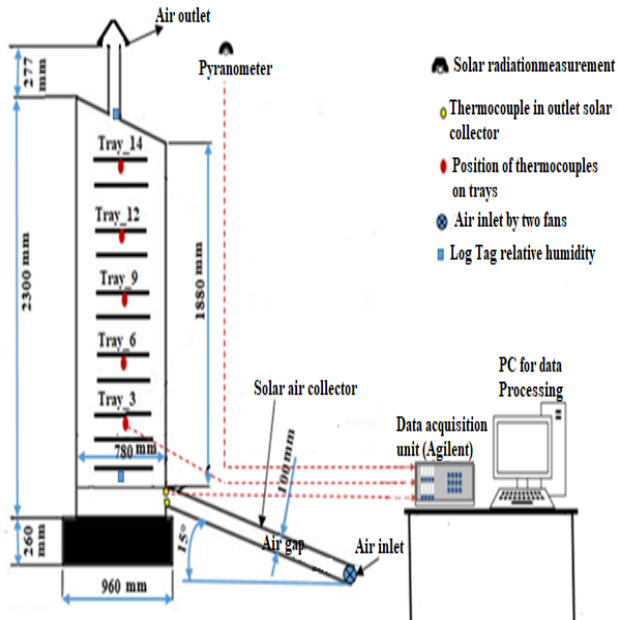


Figure 2: Measurement instrument configuration in the experimental set-up and the dimensions of the solar dryer

## II.2. Experimental set-up

A series of measurements during the experimental study was performed to characterize the thermal behaviour of the mixed solar dryer. The outdoor climatic conditions, the ambient temperature, the relative humidity of the air and the global horizontal irradiation (GHI) were measured by the meteorological station located at Ecole Supérieure Polytechnique (ESP) of Dakar.

Temperature measurements were made by thermocouples connected to the data acquisition (Agilent 34970A). A 20-connection multiplexer equips the Agilent 34970A, which is connected to a computer to store the data. The K-type thermocouples were placed at different locations in the dryer (Figure 2). To highlight the vertical stratification of the air temperature in the drying chamber, thermocouples were placed below trays 3, 6, 9, 12 and 14. Two thermocouples measured the air temperature at the outlet of the solar collector. These temperatures were measured at 10-minute intervals.

The average air temperature and relative humidity were measured with two loggers, "Log Tag". One was placed underneath tray 1 and the other was positioned in the chimney (drying chamber outlet).

The load test was carried out for the drying of 7 kg of wet mass of millet flour pellets. The product was spread evenly on the trays. The masses of trays 1, 7 and 14 were used as samples and were weighed using a digital balance (Sartorius LP 12000S). At the end of each drying experiment, the sample was placed in an oven at 105 °C for 24 hours and then weighed to determine its dry matter. The uncertainties of the measured parameters of the different measuring instruments in the experiments are presented in Table 1.

Table 1: Characteristics of measuring instruments

Measuring instruments	Uncertainties	Measuring range
Agilent 34970A data	± 0.01 °C	-

logger		
K-Type Thermocouples	± 0.1 °C	-200 to + 1300 °C
SMP10 pyranometer (Kipp&Zonen) [24]	< 2 %	0 to 4000 W/m <sup>2</sup>
Digital balance (Sartorius LP 12000S)	± 0.1 mg	0 to 12 kg
Log Tag	±0,1 °C 0,1%	-40 °C to 85 °C 0 to 100%

## II.3. Mathematical modelling of drying kinetics

The water content ( $M$ ) at each time is calculated from the following equation [11, 25]:

$$M = \frac{m_t - m_d}{m_d}$$

Where  $m_t$  et  $m_d$ , respectively represent the mass at time  $t$  and the mass of the dry matter.

The reduced water content ( $MR$ ) at time  $t$  can be calculated by the following formula [11, 25]:

$$MR = \frac{M_t - M_{eq}}{M_0 - M_{eq}}$$

$M_0$  et  $M_{eq}$ , represent respectively the initial water content and the equilibrium water content of the product on a dry basis.

However, given that  $M_{eq}$  is relatively small compared to  $M_t$  and  $M_0$  [26, 27, 28] the expression of  $MR$  can be reduced to:

$$MR = \frac{M_t}{M_0}$$

The drying rate at time  $t$  is calculated by [29]:

$$DR = - \frac{dM}{dt} = \frac{M_t - M_{t+\Delta t}}{\Delta t}$$

Where  $M_{t+\Delta t}$ , is the water content at the instant  $t + \Delta t$ . Several semi-empirical models have been proposed to represent the evolution of the reduced water content of the product. The goodness of fit of each mathematical model was assessed using the correlation coefficient ( $R^2$ ), the mean squared error (RMSE) and the mean of the sum of the squared errors ( $\square^2$ ). The most suitable drying kinetics model is the one with a higher value of  $R^2$  and lower values of RMSE and  $\square^2$ . These parameters can be calculated as follows [28]:

$$RMSE = \sqrt{\frac{\sum_{i=1}^N (XR_{exp,i} - XR_{pre,i})^2}{N}}$$

$$\square^2 = \frac{\sum_{i=1}^N (XR_{exp,i} - XR_{pre,i})^2}{N - n}$$

$$R^2 = \frac{\sum_{i=1}^N (XR_i - XR_{pre,i}) \cdot \sum_{i=1}^N (XR_i - XR_{exp,i})}{\sqrt{\left[ \sum_{i=1}^N (XR_i - XR_{pre,i})^2 \right] \cdot \left[ \sum_{i=1}^N (XR_i - XR_{exp,i})^2 \right]}}$$

Where  $MR_{exp,i}$  represents the  $i$ th value of the reduced water content obtained from the experimental results,  $MR_{pre,i}$  is the  $i$ th value of the reduced water content predicted using the model,  $N$  represents the number of measurement points, while  $n$  represents the number of drying constants in the model. Table 2 represents the semi-empirical models used to describe the thin layer drying kinetics [30, 31].

Table 2: Semi-empirical models

Models	Equations
Modified Henderson and Pabis	$MR = a \cdot \exp(-kt) + b \cdot \exp(-gt) + c \cdot \exp(-ht)$
Wang and Singh	$MR = 1 + a \cdot t + b \cdot t^2$
Two-term	$MR = a \cdot \exp(-k_0 t) + b \cdot \exp(-k_1 t)$
Midilli et al	$MR = a \cdot \exp(-kt^n) + b \cdot t$
Page	$MR = \exp(-kt^n)$
Logarithmic	$MR = a \cdot \exp(-kt) + c$
Two-term exponential	$MR = a \cdot \exp(-kt) + (1-a) \cdot \exp(-k \cdot at)$

Where  $a, b, c, g, h$  and  $n$  are empirical constants in drying models,  $k, k_0$  and  $k_1$  are empirical coefficients in drying models ( $s^{-1}$ ), and  $t$  is the drying time.

### III. Results and discussion

#### III.1. Characterization of the solar dryer under no load (without load)

The experimental studies were carried out at the Ecole Supérieure Polytechnique of the Cheikh Anta Diop University of DAKAR at latitude  $14.68^\circ$  North and longitude  $-17.47^\circ$  West. The first test consisted in characterizing the solar dryer under no load. Tests were carried out on sunny days with a clear sky (see irradiation in Figure 3), and we represent the air temperatures for March 15, 2021, as an indication. It is shown in Figure 3 the daily variation of the outside air temperature, the average air temperature in the drying chamber and the air temperature at the solar collector outlet as a function of time.

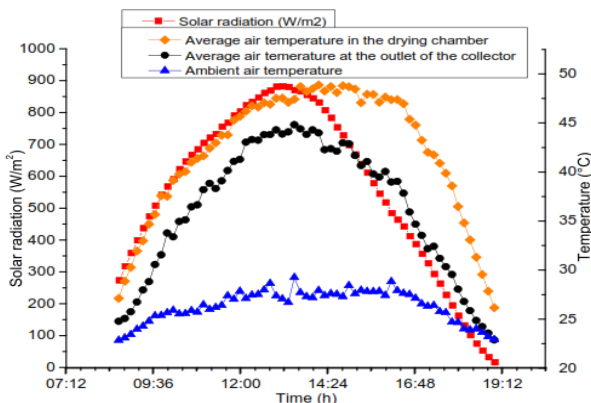


Figure 3: Variations in temperature and solar radiation as a function of time

The air temperature in the drying chamber increases from  $27.1^\circ\text{C}$  to  $48.8^\circ\text{C}$  between 8:40 and 14:00 and then decreases to  $26.2^\circ\text{C}$  at 19:00. The same observations were made at the solar collector outlet for temperature values varying between  $25.1^\circ\text{C}$  and  $44.3^\circ\text{C}$ , then decreasing to  $22.8^\circ\text{C}$ . Thus, the different temperature between the drying chamber and the ambient air can reach  $21.5^\circ\text{C}$ .

The drying chamber temperature is always higher than that of the air at the outlet of the solar collector. This is due to the heat input through the glass walls and the empty drying chamber. We note that the temperature difference between the drying chamber and the solar collector outlet is lower at the beginning than at the end of the day. This could be due to the shading of the drying chamber on the solar collector, which will lower the heated air temperature.

Figure 4 represents the variation of air temperature at different positions in the drying chamber as a function of time.

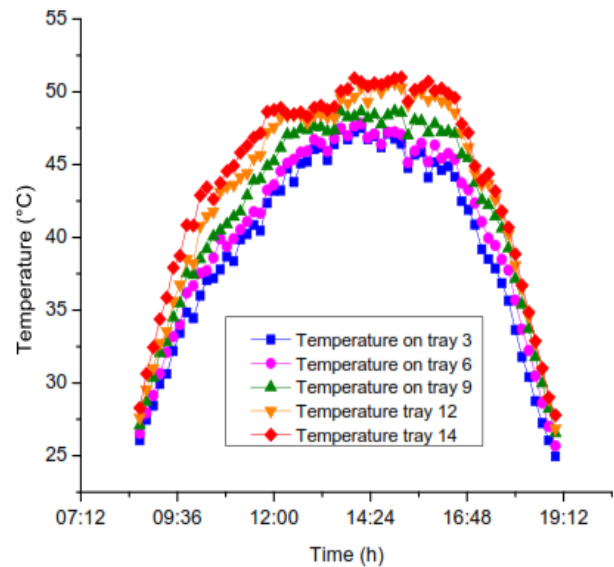


Figure 4: Temperature variations in a drying chamber under no load as a function of time

We notice a stratification of the drying chamber's air temperature, reaching a maximum value of  $6.9^\circ\text{C}$ . This shows that the air continues to heat up in the drying chamber by the direct input of solar radiation through the glass walls. The air temperature increases along the height of the drying chamber. The air temperature at the upper tray (tray 14) is always higher than at the lower trays. It reaches a maximum value of  $50.9^\circ\text{C}$  at 15:10 on the other hand, the lowest air temperature was obtained on the lower tray (tray 3), reaching a value of  $46.44^\circ\text{C}$ .

#### III.2. Characterization of the solar dryer with product (with load)

The load characterization consists in testing the drying of millet pellets in the solar dryer with a mass of 7 kg products. The load test took place on May 25, 2021, and we noted cloudy periods (see irradiation in Figure 5). Figure 5 represents the variation of the average air temperature in the drying chamber and the solar collector's outlet temperature as a function of time.

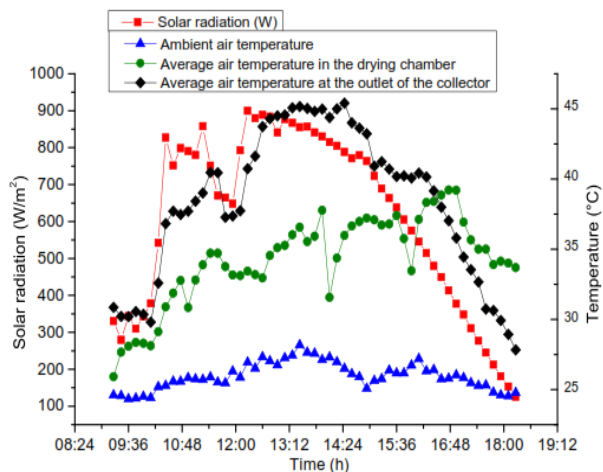


Figure 5: Temperature and radiation variations as a function of time

The outlet air temperature of the solar collector increases from 30.9 °C to 45.4 °C from 9:16 to 14:26. After this period, the outlet air temperature of the collector decreases to 27.8 °C at 18:16. The same observations were made in the drying chamber for temperature values from 25.9 °C to 34.4 °C, then decreasing to 33.7 °C. We observed a difference of temperature between the drying chamber and the ambient air that could reach a maximum value of 13.4 °C. We can note that this difference is weakly compared to the observation made during the experimental test of the unloaded case. For the period 9:16 to 16:30, the air temperature in the drying chamber is lower than that of the solar collector outlet air temperature. After 16:30, the air temperature in the drying chamber becomes higher. The air temperature increase in the drying chamber remains low because of the absorption of the sensible heat of air for extraction of the water in the product. This phenomenon creates a negative difference in temperature between the drying chamber and outlet collector air temperature. This negative temperature persists despite the direct radiation through the glass walls of the drying chamber. At the end of drying, water extraction from the product slows down. That is what shows the positive difference in temperature observed during this phase.

In Figure 6, we present the variation of air temperature at different positions in the drying chamber as a function of time.

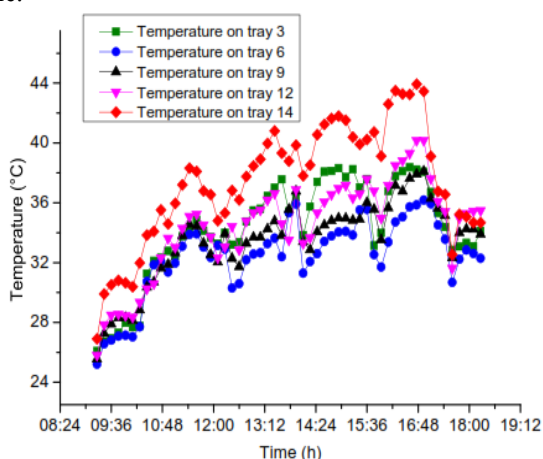


Figure 6: Temperature variations in the drying chamber with load as a function of time.

The measured air temperature at trays differs from one position to another. The temperature decreases from tray 3 to tray 6 and then rises to tray 14. The drop in temperature in the lower part of the drying chamber is explained by the significant evaporation of the water extracted from the product. This evaporation slows down as the air rises in the drying chamber. In addition, the direct contribution of solar radiation in the drying chamber explains the rise in temperature observed on the upper trays. However, no stratification of air temperature has been observed from bottom to top in the drying chamber. The highest temperatures were observed on the upper trays (trays 14, 12 and 9). The air temperature decreases from tray 14 to tray 9. This effect is noticed in direct solar dryers, where a stratification of the air temperature from top to bottom is noted. This is due to the direct contribution of solar radiation through the transparent glass walls. Y.I. Sallam *et al.* [32]. present the air temperature variations at different positions in a direct solar dryer. The results show that the air temperature increases from the lower tray to the higher tray. This is due to the greenhouse effect associated with the transparent materials (glass, plastic) which continue to heat the air rising in the drying chamber despite the heat and mass exchange that takes place between the air and the products from the lower to the upper tray. In general, there is a stratification of the air temperature from top to bottom in the drying chamber in direct mode. The lowest temperature, on the other hand, is recorded on tray 6 compared to the lower tray (tray 3). This decrease in air temperature from tray 3 to tray 6 shows that the hot air has absorbed moisture from the products on the lower trays and passed to tray 6. This phenomenon may be seen in the instance of indirect solar dryers, where a stratification of the temperature from the bottom to the top is noted. V.R. Mugi *et al.* [16]. present the variations of the air average temperature at different locations in an indirect solar dryer with forced convection. The results show that the air temperature decreased from the lower to the upper tray. This explains a cooling phenomenon of the air exchanging its heat with the products of the lower tray through the upper trays. The stratification of the air temperature takes place from the bottom to the top.

Figure 7 shows the variation of the relative air humidity at the position of the tray 1 and at the inlet to the chimney as a function of time. It can be seen that the relative air humidity decreases as the temperature in the drying chamber increases.

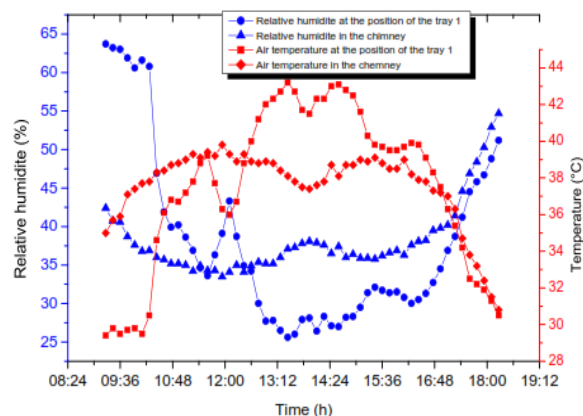


Figure 7: Variation of the relative humidity of the air in the dryer as a function of time

At the beginning, the maximum value of 64% of relative humidity is recorded at the position of tray 1, which is marked by the low temperature value of 29.4 °C. The evaporation of water from the product favours the phenomenon of water stream diffusion in the drying air, which results in a rise in relative humidity at the beginning. Afterwards, a decrease in relative humidity until 25% has been observed, which is due to the effect of the increase in air temperature. At the level of the chimney, the relative air humidity remains low until 12:36. After that, it becomes higher than the relative humidity at the level of the tray 1. This can be justified by the increase in air temperature at the level of the tray 1 due to the heat input from the solar collector. The chimney effect favours the extraction of the air humidified by the product towards the outside.

### III.3. Results of the drying kinetics of millet pellets

We studied the drying kinetics of millet pellets at different positions in the drying chamber. We present in Figure 8 the variation of the reduced water content of the product as a function of time for samples from trays 1, 7 and 14.

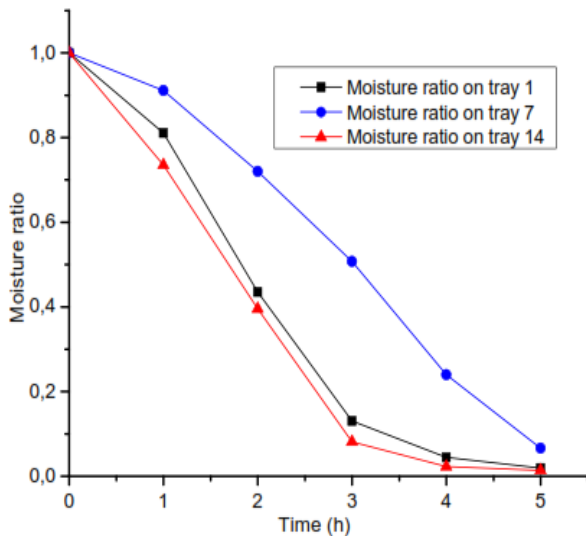


Figure 8: Variation of the product's reduced water content as a time function.

We observe that the reduced water content of the millet pellets of trays 1 and 14 decreases very quickly and then slows down. On tray 1, a decrease in the water content is noted, reduced from 1 to 0.13 in 3 hours and going from 0.13 to 0.01 in 2 hours. On the one hand, at the tray 7 level, the decrease in the reduced water content is slighter. The reduced water content goes from 1 to 0.5 in 3 hours and from 0.5 to 0.06 in 2 hours. The drying speed of trays 1 and 14 is greater than that of tray 7 because the former benefit either from the collector's heat input or the direct solar input into the drying chamber. On the other hand, tray 7 located in the middle of the drying chamber, is crossed by air already loaded with humidity and shaded by the upper trays. There is an inversion of the product drying speed between the middle tray (tray 7) and the trays above (tray 14) and below (tray 1) in this mixed solar dryer.

However, this differs in the case of a direct or indirect solar dryer. The variation in reduced water content of the product in a direct solar dryer show that the upper tray

dries faster than the lower trays [32]. There is a decrease in the drying rate from the upper to the lower tray. This explains the direct nature of the solar dryer, which allows the sun's rays to pass through. Thus, the upper tray benefits from this direct sunlight compared to the others. The lower tray dries less quickly than the other trays, because it is shaded by the trays above it. This phenomenon is only observed in the case of a direct solar dryer. In the case of indirect solar dryer [16], the variations of product moisture content show that the trays close to the collector dry faster than the trays further away. The drying speed decreases of the tray closer to the collector towards the other trays. This phenomenon may be seen in the instance of an indirect solar dryer.

This difference in results is due to the type of dryer and the variation of the drying process conditions.

The variations of the reduced water content of the product as a function of time are used to evaluate by non-linear regression analysis different models to identify the best mathematical model describing the drying kinetics of millet pellets. The results of the fitting coefficients of different models as well as the parameters  $R^2$ ,  $\chi^2$  and RMSE are given in tables 3, 4 and 5, respectively, for trays 1, 7 and 14.

Table 1: Fitting parameters of the different models for thin-layer solar drying of millet pellets at tray level 1.

Model name	Coefficients and constants	$R^2$	$\chi^2$	RMSE
Henderson and Pabis	a = -2.95772; b = 2.01228; c = 2.01225; k = 0.317116; g = 0.35687; h = 0.3557	0.9415	0.02154	0.14677
Wang and Singh	a = 0.33373; b = 0.02764	0.9432	0.00089	0.09465
Two term	a = 0.0754; b = 0.99701; k <sub>0</sub> = 0.49844; k <sub>1</sub> = 0.49836	0.9383	0.01364	0.11678
Midilli et al	a = 1; b = 0.01445; k = 0.2273; n = 56.34836	0.8277	0.03809	0.19516
Page	k = 0.20905; n = 2.01894	0.9775	0.00354	0.05949
Logarithmic	a = 1.08979; c = -0.02134; k = 0.47303	0.9391	0.01122	0.10591
Two term	a =	0.9322	0.0107	0.1034

exponentie l	0.99875 k = 0.45823	3		6
-----------------	---------------------------	---	--	---

exponentiel	k = 0.1			
-------------	---------	--	--	--

**Table 42: Fitting parameters of the different models for thin-layer solar drying of millet pellets at tray level 7.**

Model name	Coefficients and constants	R <sup>2</sup>	χ <sup>2</sup>	RMSE
Henderson and Pabis	a = 0.091; b = 0.298; c = 0.731; k = 0.3295; g = 0.3294; h = 0.3298	0.9264	0.0300	0.1734
Wang and Singh	a = -0.216 ; b = 0.011	0.9565	0.0076	0.0872
Two term	a = 0.3657; b = 0.7549; k <sub>0</sub> = 0.32955; k <sub>1</sub> = 0.32973	0.9264	0.0180	0.1343
Midilli et al	a = 0.8072; b = -0.1125; k = -0.2377; n = -9.4674 10 <sup>10</sup>	0.1183	0.2162	0.4649
<b>Page</b>	<b>k = 0.0801; n = 2.0296</b>	<b>0.9908</b>	<b>0.0016</b>	<b>0.0400</b>
Logarithmic	a = 1.4478; c = -0.36759; k = 0.18598	0.9568	0.0088	0.0938
Two term exponentiel	a = 2.2619; k = 0.52158	0.9832	0.0029	0.0542

**Table 5: Fitting parameters of the different models for thin-layer solar drying of millet pellets at tray level 14.**

Model name	Coefficients and constants	R <sup>2</sup>	χ <sup>2</sup>	RMSE
Henderson and Pabis	a = -0.6878; b = 0.8439; c = 0.8439; k = 132.55; g = 0.8135; h = 0.8135	0.9783	0.0077	0.0879
Wang and Singh	a = -0.3539; b = 0.0302	0.9472	0.0081	0.0897
Two term	a = 0.0773; b = 0.9788; k <sub>0</sub> = 0.5539; k <sub>1</sub> = 0.5538	0.9493	0.0108	0.1041
Midilli et al	a = 0.9513; b = -0.4336; k = -0.1557; n = 1.0298	0.9251	0.0160	0.1265
<b>Page</b>	<b>k = 0.2806; n = 1.8571</b>	<b>0.9825</b>	<b>0.0026</b>	<b>0.051</b>
Logarithmic	a = 1.0718; c = -0.0188; k = 0.5281	0.9502	0.0088	0.094
Two term	a = 0.9984	0.8682	0.2853	0.5341

When we compare the parameters R<sup>2</sup>, χ<sup>2</sup> and RMSE, we can say that the Page model is the best model describing the drying of millet pellets in the thin layer mixed solar dryer. This result is different from P.T. Bassene *et al.* [19] on the same product. This difference in result could be explained by the drying conditions, which are not identical. Thus, Page's model developed in this work is more realistic for the solar drying of millet pellets. Similarly, similar findings have been reported in the literature. For thin-layer pepper drying, A. Zaineb *et al.* [29] showed that the kinetics of drying in the open air or inside a greenhouse without MCP is described by the Two-term model, whereas that of drying inside a greenhouse with MCP is the model of Midilli *et al.*

### III.4. Comparison of experimental and numerical values

Figure 9 presents the regression curve between the semi-empirical model and the experimental values of the reduced water content of the product.

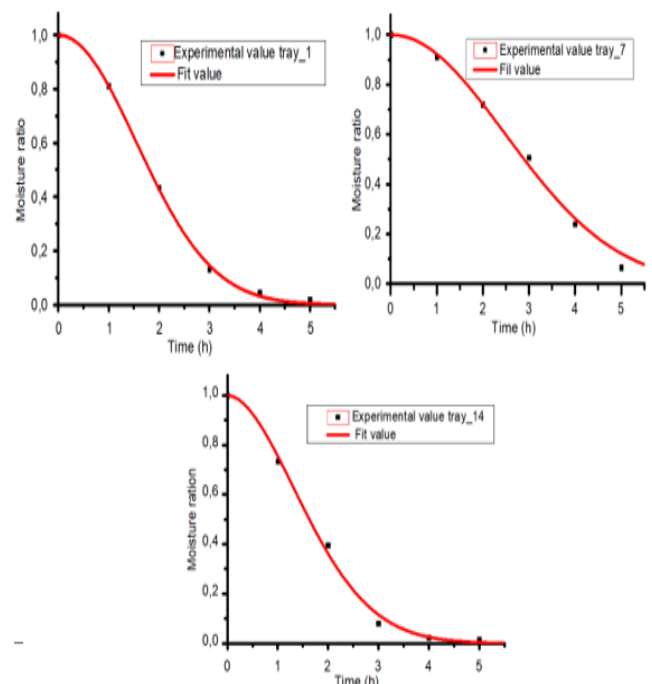


*Figure 9: Simulated and measured moisture ratio*

We notice that the results obtained by the model are pretty close to those obtained by the observations. There is a perfect alignment between the experimental and predicted values of the reduced water content of millet pellets on the position of trays 1 and 14. The performance of the simulation was determined using the coefficient (R<sup>2</sup>) by comparing the values of the observed and predicted reduced water content. The correlation coefficient results are respectively 0.9991, 0.9942 and 0.999 for trays 1, 7 and 14 for the Page model.

### IV. Conclusion

In this work, a mixed solar dryer with forced convection has experimentally been characterized without product

and with product for the drying of millet pellets. The kinetics of thin film drying of millet pellets have been studied in the dryer. And by non-linear regression analysis, different models were evaluated to identify the best mathematical model describing the drying kinetics of millet pellets. In conclusion, the results of this work are expressed as follows:

- The characterization of the solar dryer under no load showed that the air temperature in the drying chamber could reach a maximum value of 48.8 °C, which is a difference of 21.5 °C from the outside air temperature. A stratification of the drying chamber's air temperature is observed, reaching a maximum value of 6.9 °C.
- The test of the solar dryer with load for drying millet pellets shows an air temperature in the drying chamber with a maximum value of 34.4 °C, that is a difference of 13.4 °C with the outside air temperature. At the beginning of the drying process, the air temperature increase in the drying chamber remains low due to the absorption of the sensible heat of air for extraction of the water in the product. This phenomenon creates a negative difference in temperature between the drying chamber and outlet collector air temperature. At the end of drying process, water extraction from the product slows down. This explains the positive difference in temperature observed during this phase. However, no air temperature stratification was observed in the drying chamber. Two phenomena were observed in this mixed solar dryer during the drying of millet pellets. The highest temperatures are observed at the upper trays (14, 12 and 9), showing its direct behavior. The lowest temperature, on the other hand, is observed at the level of the trays located in the middle in relation to the lower tray (tray 3), which shows its indirect behavior.
- The drying kinetics of the millet pellets showed that the lower and upper trays dried faster than the intermediate (middle) trays, and the product was dried in 5 hours. Of all the mathematical models considered in this study to approximate the kinetics of thin-film drying, Page's model best describes the drying of millet pellets in the mixed solar dryer.

### References

- [1] Hany S.EL-Mesery, Improving the thermal efficiency and energy consumption of convective dryer using various energy sources for tomato drying, Alexandria Engineering Journal 61 (2022) 10245-10261.
- [2] Greg Wheatley et Robiul Islam Rubel, «Design improvement of a laboratory prototype for efficiency evaluation of solar thermal water heating system using phase change material (PCMs),» Results in Engineering 12 (2021) 100301.
- [3] El HadjiI. Cisse, Ababacar Thiam, Baye Alioune Ndiogou, Dorothé Azilinson et Vincent Sambou, «Experimental investigation of solar chimney with concentrated collector (SCCC),» Case Studies in Thermal Engineering 35 (2022) 101965.
- [4] J.K. Afriyie , M.A.A. Nazha , H. Rajakaruna et F.K. Forson, «Experimental investigations of a chimney-dependent solar crop dryer,» Renewable Energy 34 (2009) 217–222.
- [5] O. V. EKECHUKWU et B. NORTON, «Design And Measured Performance of a Solar Chimney for Natural-Circulation Solar-Energy Dryers,» Renewable Energy 10 (1997) 81-90.
- [6] H. Krabch, R. Tadili et A. Idrissi, «Design, realization and comparison of three passive solar dryers. Orange drying application for the Rabat site (Morocco),» Results in Engineering 15 (2022) 100532.
- [7] S. K. DAS et Y. KUMAR, «Design and Performance of a Solar Dryer With Vertical Collector Chimney Suitable for Rural Application,» Energy Conversion and Management 29 (1989) 129-135.
- [8] Andre G. FERREIRA, Cristiana B. MAIA, Marcio F.B. CORTEZ C et Ramon M. VALLE, «Technical Feasibility Assessment of a Solar Chimney for Food Drying,» Renewable Energy, 34 (2009) 217-222.
- [9] A. Fudholi, K. Sopian, M.H. Ruslan et M.A. Alghoul, «Review of solar dryers for agricultural and marine products,» Renewable and Sustainable Energy Reviews 14 (2010) 1–30.
- [10] Pimpan Pruengam, Siwalak Pathaveerat et Prasertsak Pukdeewong, «Fabrication and testing of double-sided solar collector dryer for drying banana,» Case Studies in Thermal Engineering 27 (2021) 101335.
- [11] Aymen EL khadraoui, Ilhem Hamdi, Sami Kooli et Amenallah Guizani, «Drying of red pepper slices in a solar greenhouse dryer and under open sun : Experimental and mathematical investigations,» Innovative Food Science and Emerging Technologies 52 (2019) 262–270.
- [12] Khalil E.J. Al-Juamily, Abdul Jabbar N. Khalifa et Tadahmun A. Yassen, «Testing of the performance of a fruit and vegetable solar drying system in Iraq,» Desalination 209 (2007) 163–170.
- [13] Melike Sultan Karasu Asnaz et Ayse Ozdogan Dolcek, «Comparative performance study of different types of solar dryers towards sustainable agriculture,» Energy Reports 7 (2021) 6107–6118.
- [14] V. Subbian, K. Kalidasa Murugavel, R. Satheesh Raja et A.M. Shanawaz, «Experimental investigation and the performance evaluation of a mixed mode solar dryer for coconut,» Materials Today : Proceedings 45 (2021) 3662-3665.

- [15] Hany S.EL-Mesery, Nermeen M.Tolba et Reham M.Kamel, Mathematical modelling and performance analysis of airflow distribution systems inside convection hot-air dryers, Alexandria Engineering Journal 62 (2023) 237-256.
- [16] V. R. Mugi et C. V.P, «Energy, exergy and economic analysis of an indirect type solar dryer using green chilli: A comparative assessment of forced and natural convection,» Thermal Science and Engineering Progress 24 (2021) 100950.
- [17] Mohammadhossein Rezaei, Mohammad Sefid, Khalid Almutairi, Ali Mostafaeipour, Hoa Xuan Ao, Seyyed Jalaladdin Hosseini Dehshiri, Seyyed Shahabaddin Hosseini Dehshiri, Shahariar Chowdhury et Kuaanan Techato, «Investigating performance of a new design of forced convection solar dryer,» Sustainable Energy Technologies and Assessments 50 (2022) 101863.
- [18] Ngoné Fall Beye, Cheikhou Kane, Nicolas Ayessou, Cheikh Mouhamed Fadel Kebe, Cheikh Talla, Codou Mar Diop et Abdou Sène, «Modelling the dehydration kinetics of four onion varieties in an oven and a solar greenhouse,» Heliyon 5 (2019) e02430.
- [19] P. T. Bassene, S. Gaye, A. Talla, V. Sambou et D. Azilinson, «Experimental and modelling study of thin layer drying kinetics of pellets millet flour,» African Journal of Agricultural Research, Vol. 8(28), pp. 3806-3813, 26 July, 2013.
- [20] Khuthadzo Mugodo et Tilahun S. Workneh, «The kinetics of thin-layer drying and modelling for mango slices and the influence of differing hot-air drying methods on quality,» Heliyon 7 (2021) e07182.
- [21] K. Turhan, «An Investigation on the performance Improvement of greenhouse-type agricultural dryers,» Renewable Energy 31 (2006) 1055–1071.
- [22] P. Nimnuan et S. Nabnean, «Experimental and simulated investigations of the performance of the solar greenhouse dryer for drying cassumunar ginger (Zingiber cassumunar Roxb.),» Case Studies in Thermal Engineering 22 (2020) 100745.
- [23] Siyabonga Gasa, Siphosibanda, Tilahun S.Workneh, Mark Laing et Alaika Kassim, «Thin-layer modelling of sweet potato slices drying under naturally-ventilated warm air by solar-venturi dryer,» Heliyon 8 (2022) e08949.
- [24] Ababacar NDIAYE, Etude de la dégradation et de la fiabilité des modules photovoltaïques Impact de la poussière sur les caractéristiques électriques de performance, Dakar: Université Cheikh Anta DIOP de DAKAR de Ecole Supérieure Polytechnique, 2012-2013.
- [25] Ilhem HAMDI, Sami KOOLI, Aymen ELKHADRAOUI, Zaineb AZAIZIA, Fadhel Abdelhamid et Amenallah GUIZANI, «Experimental study and numerical modeling for drying grapes under solar greenhouse,» Renewable Energy 127 (2018) 936-946.
- [26] Kamil Sacilik et Ahmet Konuralp Elicin, «The thin layer drying characteristics of organic apple slices,» Journal of Food Engineering 73 (2006) 281–289.
- [27] A.O. Dissa, D.J. Bathiebo, H. Desmorieux, O. Coulibaly et J. Kouliadiati, «Experimental characterisation and modelling of thin layer direct solar drying of Amelie and Brooks mangoes,» Energy 36 (2011) 2517-2527.
- [28] D.V.N.Lakshmi, P.Muthukumar, Apurba Layek et Prakash Kumar Nayak, «Drying kinetics and quality analysis of black turmeric (Curcuma caesia) drying in a mixed mode forced convection solar dryer integrated with thermal energy storage,» Renewable Energy 120 (2018) 23-34.
- [29] Zaineb Azaizia, Sami Kooli, Ilhem Hamdi, Wissem Elkhali et Amen Allah Guizani, «Experimental study of a new mixed mode solar greenhouse drying system with and without thermal energy storage for pepper,» Renewable Energy 145 (2020) 1972-1984.
- [30] E. Kavak Akpınar et Y. Bicer, «Mathematical modelling of thin layer drying process of long green pepper in solar dryer and under open sun,» Energy Conversion and Management 49 (2008) 1367–1375.
- [31] Jasinta Poonam Ekka et Muthukumar Palanisamy, «Determination of heat transfer coefficients and drying kinetics of red chilli dried in a forced convection mixed mode solar dryer,» Thermal Science and Engineering Progress 19 (2020) 100607.
- [32] Y.I. Sallam, M.H. Aly, A.F. Nassar et E.A. Mohamed, Solar drying of whole mint plant under natural and forced convection, Journal of Advanced Research (2015) 6, 171–178.

Soumaila TIGAMPO<sup>(a)</sup>, El Hadji I Cisse<sup>(a)</sup>,  
Ababacar THIAM<sup>(a,b)</sup>, Panel Thierry BASSENE<sup>(a)</sup>,  
Vincent SAMBOU<sup>(a)</sup>

<sup>(a)</sup>Laboratoire Eau-Énergie-Environnement-Procédés Industriels (LE3PI)/UCAD/ESP

<sup>(b)</sup>Université Alioune Diop de Bambey